opción

Revista de Antropología, Ciencias de la Comunicación y de la Información, Filosofía, Lingüística y Semiótica, Problemas del Desarrollo, la Ciencia y la Tecnología

Año 35, diciembre 2019 Nº 24
Revisten de Ciencias Humanas y Sociales
ISSN 1012-1587/ ISSNe: 2477-9385
Depósito Legal pp 198402ZU45

Universidad del Zulia
Facultad Experimental de Ciencias
Departamento de Ciencias Humanas
Maracaibo - Venezuela

Opción, Año 35, Regular No.24 (2019): 1134-1154
ISSN 1012-1587/ISSNe: 2477-9385

Assessment of Sand Dune Hazards for Land Use/Land cover in Ma'an Governorate

Aymen AL-Taani[1]
[1]Al-Hussein Bin Talal University College of Arts, Department: of History and Geography, Jordan.
Email: ayman.a.taani@ahu.edu.jo

Yusra Al-husban[2]
[2]Department of Geography, Faculty of Arts, the University of Jordan, Amman, Jordan.
Email: y.alhusban@ju.edu.jo

Abstract

The main goals of this paper are to assess the risk of sand accumulation as a hazard for the land use/land cover (LULC) in Ma'an Governorate via comparative quantitative research methods. The results of LULC showed that human activities represent only 340.74 km² (1.03%), namely of built-up area, forest and irrigated area, besides the 240 km of road length concentrated in the western and southwestern regions of Ma'an, so the sand accumulation is hazards well-studied in detail in this area. In conclusion, many farms were relocated from one place to another to avoid areas covered by sand dunes.

Keywords: Sand Dune, Hazards, LULC, Ma'an Governorate.

Recibido: 10-11-2018 •Aceptado: 10-03-2019

Evaluación de los peligros de las dunas de arena para el uso de la tierra / cobertura de la tierra en la gobernación de Ma'an

Resumen

Los objetivos principales de este documento son evaluar el riesgo de acumulación de arena como un peligro para el uso del suelo / cobertura del suelo (LULC) en la gobernación de Ma'an a través de métodos de investigación cuantitativa comparativa. Los resultados de LULC mostraron que las actividades humanas representan solo 340.74 km² (1.03%), a saber, del área edificada, el bosque y el área irrigada, además de los 240 km de longitud de la carretera concentrados en las regiones oeste y suroeste de Ma'an, por lo que La acumulación de arena es un peligro bien estudiado en detalle en esta área. En conclusión, muchas granjas fueron reubicadas de un lugar a otro para evitar áreas cubiertas por dunas de arena.

Palabras clave: Duna de arena, Peligros, LULC, Gobernación de Ma'an.

1. INTRODUCTION

Ma'an Governorate occupies ca. (37%) of the total area of Jordan, and most of it is area classified as hyper-arid land (89.2%), with annual precipitation less than 50mm/y. Sand dunes occupy 6226.79 km², some 18.9 % of the total area of Ma'an Governorate, as measured by Landsat ETM+ 2018. According to the wind speed and direction, the dunes move at different rates and in different directions, and the dynamic nature of sand dunes and their potential hazards for the main human activities in Jordan have been reported only in the

case of Wadi Araba. This kind of natural hazard is widely studied around the world using different methodologies (KHIDR, 2006; EL-BAZ, 1998).

This was conducted over a wide area of Ma'an Governorate, concentrated in the western and southwestern part of the study area with high potential hazards for land use. In this paper, five spatial digital maps were used. These factors are then overlaid considering their importance based on the weight accorded to each factor. The final output of this analysis is a map that shows the areas that are prone to sand dune with the degree of the proneness specified, categorized as follows: very low, low, moderate, high, and very high.

Ma'an is located in the southern part of Hashemite Kingdom of Jordan (HKJ) and extends between longitudes 35° 30´ to 38° 00´ E and latitudes 29° 00´ N to 31° 30´ (see Figure 1). Ma'an forms the Jordanian-Saudi border over a distance of 744 km, and has the largest area of the 12 governorates, with an estimated population of 152,000 in 2018. It has the lowest population density in Jordan: about 1.27 persons per square km. Ma'an has largely a desert climate, but the western highlands have a Mediterranean climate. Consequently, the western highlands area of Ma'an is of special importance because it is marked by the highest precipitation and is where most human activities are concentrated (JAMLI, ZAREKIA & RANDHIR, 2018).

Rainfall is scarce and the average annual rainfall ranges from < 50 mm in the East and Qa'a Al-Jafer, which forms 29,450.2 ,km² (89.2%), to 350 mm/y in a small portion of 163.05 km² (0.49 %) in the Western Highlands, while the rest of the study area (10.3%), with

mean rainfall, ranges from 250 to 100 mm/y. Ground elevation is between 262 m to 1710 m in the Western Highlands, while the mean elevation is 986 m. and (77.8%) of the total area has an elevation between 262 m and 932 m, with relief of 1,448 m. Slope terrain (80.3%) of the total area is nearly level, and only 2.8% of the total area is moderate to the steep slope (see Figure 3).

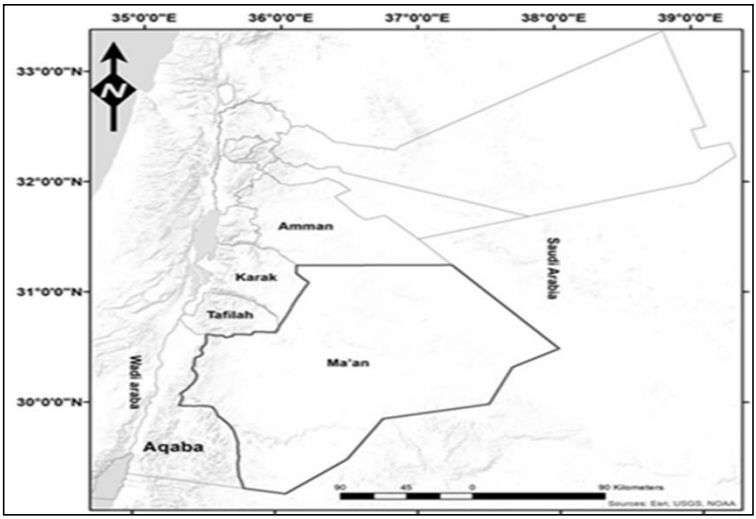

Figure. 1: Location map of the study area.

2. METHODOLOGY

In order to achieve the study goal, Satellite images of Landsat 4, 5 Thematic Mapper (TM) and Landsat 8 Operational Land Imager (OLI)/ were acquired from United States Geological Survey (USGS)

website; Landsat TM and OLI were selected to represent the governorate. The land use/cover (LULC) maps were extracted for detecting different changes in LULC during the period 1990 to 2018 and then used to generate the risk map of sand dunes for the Ma'an Governorate (LIVINGSTONE, WIGGS & WEAVER, 2007).

Risk assessment of sand dunes, applying GIS tools, including overlaying five spatial maps, was conducted utilizing various sources such as climatic data, DEM, and Landsat 8-OLI. The procedure model was used to analyze the key variables influencing sand dune movement in the governorate. Previous studies have documented how sand encroachment and dune movements are greatly influenced by certain environmental factors such as wind speed, wind direction, sand availability or the morphology of sand dunes (AQL, 2004; FADHIL, 2016).

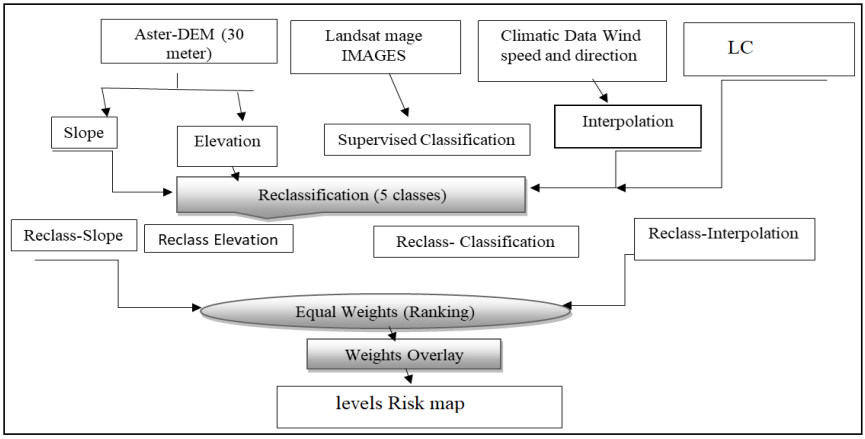

Figure 2: Flowchart for production of the sand dune risk map.

The weighted overlay in Arc Map was applied to produce the final hazard map according to the influence percentage for each layer; therefore, each layer contributes to the influence according to its influence percentage, as shown in Tables 1-2 and Figures 3-4. Different criteria are used for sand dunes classes.

Table 1: Parameters controlling the sand dune

Elevation (m)	Area (km^2)	Area (%)
262-761	7342.2	22
762-932	17621.2	52.8
933-1182	6507.8	19.5
1183-1710	1902.3	5.7
Total area (km^2)	33373.4	100
Slope (degree)	Area (km^2)	Area (%)
0 - 2	22593.8	67.7
2.1-5	9811.8	29.4
5.1-11	734.2	2.2
11.1-72	200.2	0.6
Total area (km^2)	33373.4	100
Mean annual wind speed (k/h)	Area (km^2)	Area (%)
< 5	1949.6	30.8
5-8	5339.7	16
9-12	15818.9	47.4
>12	1935.7	5.8
Total area (km^2)	33373.4	100

Land cover (LC)	Area (km^2)	Area (%)
Basalt and mud flat	8705.68	26.4
Sand dunes and sandstone	10277.49	31.1
Limestone	6891.38	20.9
Gravel	6861.62	20.8
Total area (km^2)	**32736.17**	**99.2**

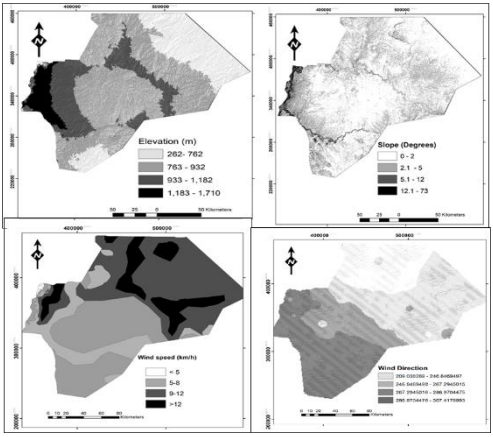

Figure 3: Elevation (m), Slope (Degrees) maps extracted from aster-DEM (30 meters), Wind speed and direction.

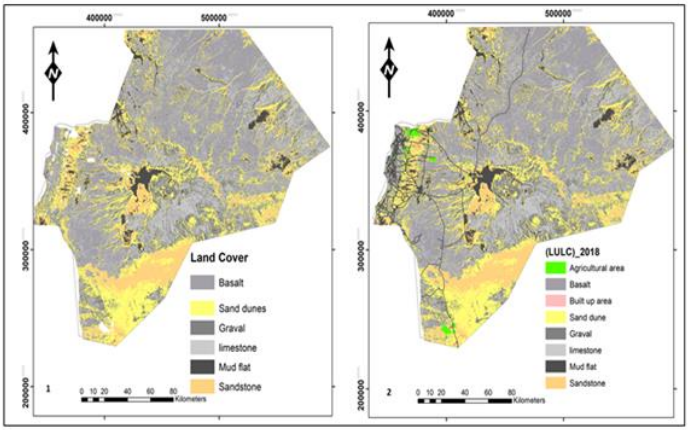

Figure 4: LC and LULC 2018

Table 2: Five parameters affecting sand dune encroachments defined as its percentage of influence

Layers according to influence percentage	Influence (%) of sand dunes hazard map
Elevation (m)	10
Slope (%)	25
Wind speed (km)	30
Wind direction	25
Land cover patterns	20
Total	100

The higher wind speed activates sand dune movement. The strongest wind covered about 5.8% of the total area of Ma'an, occurring in March 12.8 km/h, February 12.4 km/h, January 10.4km/h, and April, followed by October, November, and December. Given the

hyper-arid conditions and scarce vegetation cover, wind systems in the area are capable of producing sand dunes in different forms and directions. These sand dunes occur in association with the major valley floors and playa basins and are commonly moving against or into the foothills of the escarpments in the study area. The weakest winds in the region covered about 30.8% of the total area of Ma'an, with spatial concentrated in Qa'a Al-Jafer. The prevailing wind directions are ESE, SE, SSE, and NW, with a range from 200- 350 degrees.

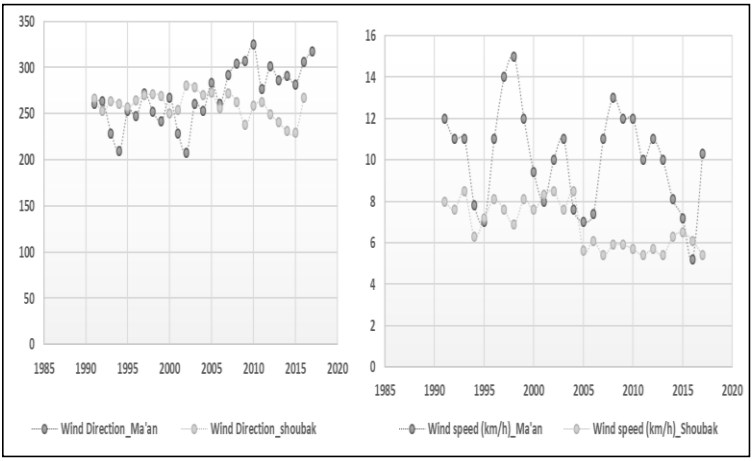

Figure 5: Annual prevailing wind speed, direction for Shoubak and Ma'an meteorological stations, obtained from the Jordan Meteorological Department.

The study area is principally comprised of barren land, ca. 32,658.43 km² (99%) of its total area, and divided into six categories according to its lithology origin. These are: mud flat (playa basins) (3.9%), the flat-floored bottom of an undrained desert basin that turns

into a shallow lake during rainy months, basalt rocks (22.5%), limestone rocks, gravel deposits (20.6%), and the rest are sand dunes and sandstone (31.1%).

To map changes that had occurred between the different dates, all spectral bands from the TM digital data were individually used as input for the purpose of supervised classification. A maximum-likelihood algorithm was used for LULC mapping from Landsat images. In total, eight (LULC) classes were included in the scheme: built-up area, forest, and irrigated area, and bare land. The barren area was classified into six layers according to its lithology: sand dune, mud flat, sandstone rocks, and basalt rocks. These eight categories of LULC changes are summarized in Table 4. In the current study risk assessment of sand dunes, applying GIS tools including overlaying five spatial maps were acquired from various sources such as LULC, topographic data, and wind speed and direction for sand dune risk modeling.

Table 3: The Parameter Risk Levels

Parameters	Risk Levels			
	1	2	3	4
Elevation (m)	262-761	762-932	933-1182	1183-1710
Slope (Degree)	0 - 2	5-8	8-15	< 8
Mean annual	< 5	5-8	9-12	>12

Wind speed (km/h)				
Land Cover	basalt rocks, mud flat, gravel deposits	limestone rocks	sandstone rocks	sand dunes

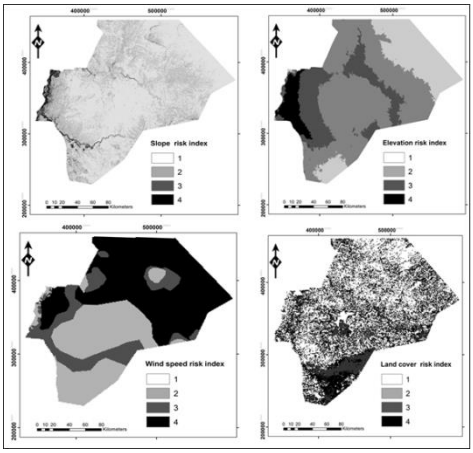

Figure 6: The Risk Levels for Each Parameter

3. RESULTS

Landsat satellite scenes, imaged during the years 1990, 2000 and 2018 were used to classify different LULC classes in the study area. According to the study, the actual number of classes identified in

this large area was highly heterogeneous in terms of geological, topographic and climatic conditions. This is a huge area and heterogeneous landscape; eight main classes could with difficulty be identified. The data obtained indicate that the LULC classes are as follows: forest and irrigated area, built-up area, and bare land. The bare area is classified according to the lithological characteristics into five types: basalt rocks, sandstone rocks, limestone rocks, gravel deposits, sand dunes, and mud flat, which covered 32736 km² (99.9%) of the total area of Ma'an Governorate. The urban class covers a small area of 340.74 km², concentrated in the western parts of the study area. The class of sand dunes covers an area of 6226.79 km², and refers to all kinds of sand accumulation. The developed areas are highly concentrated in the western and southwestern regions of Ma'an Governorate. Our case study will be in this part of the study area for risk assessment impacting on the LULC.

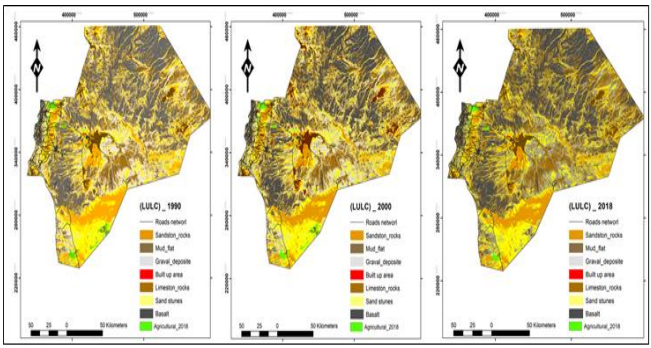

Figure 7: LULC classes of Ma'an Governorate/Jordan, based on Landsat 1990, 2000 and 2018 images, respectively

Table 4: LULC classes in this study during the study period

LULC 1990				LULC 2000		1990-2000	LULC 2018		2018-2000
No	LULC	Area km²	Area %	Area km²	Area %	Area %	Area km²	Area %	Area %
1	Forest and irrigated area	280.39	0.8	269.43	0.8	-11.0	172.36	0.5	-97.1
2	Built-up area	60.35	0.2	72.06	0.2	11.7	90.63	0.3	18.6
3	Mud flat	1292.24	3.9	1292.24	3.9	0.0	1292.24	3.9	0.0
4	Basalt rocks	7413.44	22.5	7413.44	22.5	0.0	7413.44	22.5	0.0
5	Sand dunes	6226.79	18.9	6228.12	18.9	1.3	6235.42	18.9	7.3
6	Sandstone rocks	4037.06	12.2	4037.06	12.2	0.0	4042.07	12.2	5.0
7	Limestone rocks	6891.38	20.9	6891.38	20.9	0.0	6891.38	20.9	0.0
8	Gravel deposits	6797.52	20.6	6795.43	20.6	-2.1	6861.62	20.8	66.2
Total Area km²		32999	100	32999	100		32999	100	

Accuracy assessment is necessary for testing the accuracy of the resultant classes from the classification images. There are several

methods of performing an accuracy assessment, such as the overall accuracy and the Kappa coefficient. The confusion of error matrix which can be used as a starting point for a series of descriptive and analytical statistical analyses has been used to represent the accuracy assessment.

In order to obtain the confusion matrix, random sampling was carried out. The columns of the matrix represent the reference data, while the rows indicate the classes generated from the classification process. According to previous studies, there are many ways to improve the interpretation of the confusion matrix. Among them, the Kappa coefficient is one of the most popular measures for addressing the difference between the actual agreement and the chance agreement. The Kappa coefficient of agreement was computed as follows: Where r is the number of rows in the confusion matrix,

$$\hat{k} = \frac{N\sum_{i=1}^{r} X_{ii} - \sum_{i=i}^{r}(X_{i+} \times X_{+i})}{N^2 - \sum_{i=i}^{r}(X_{i+} \times X_{+i})}$$

Where: $r\ is\ the\ number\ of\ rows\ in\ the\ confusion\ matrix$;

Xii is the number of observation in row and column I;

X + i is the total number of observation in row I;

Xi+ is the total number of observation in column I;

N is the total number of observations included in the matrix.

Tables 5 and 6 show the confusion matrices resulting from the digital data classified. For 1990, 214 GCPs were selected, which were then checked with reference to 1:50 000 topographic maps. The result shows an overall accuracy of 88%. In terms of producer accuracy, all

classes were over 77%. In terms of user's accuracy, all classes were over 83%, and a Kappa index of agreement of 0.85 was obtained. For the 2000 LULC map, 214 GCPs were selected. The result indicated an overall classification accuracy of ca. 85%. In terms of producer accuracy, all classes were over 70%. For 2018, in terms of user's accuracy, all classes were over 86%, and a Kappa index of agreement of 0.85 was noted.

A comparison of Tables 2 and 3 reveals that the 1990 LULC map is compatible inaccuracy in every respect with the 2000 LULC map, where the overall accuracy is more than 85% for both maps, indicating that this is good evidence that the image processing approach adopted in this study has been effective in producing compatible LULC data over time. In regard to producer accuracy for the 2018 LULC map, all classes were over 86%, while in terms of user's accuracy; all classes were over 83%, and a Kappa index of agreement of 0.86 was obtained. (see Table 5).

Table 5: Confusion matrix of the signatures derived from supervised training, TM 1990, 2000 and 2018.

No	Land use	Agricultural land	Built-up area	Mudflat	Basalt rocks	Basalt rocks	Sandstone rocks	Limestone rocks	Gravel deposit	Total
1	Agricultural land	18	0	0	0	0	1	1	0	20

2	Built-up Area	0	24	2	1	1	0	0	0	28
3	Mud flat	0	0	8	0	0	0	1	0	9
4	Basalt rocks	1	1	0	34	1	1	2	0	73
5	Sand dunes	1	0	0	1	34	0	1	1	5
6	Sandstone rocks	0	1	0	0	0	19	0	1	21
7	Limestone rocks	0	0	0	2	2	0	28	2	34
8	Gravel deposits	0	1	0	1	1	1	0	20	24
Total		20	27	10	39	39	22	33	24	214

Change detection and monitoring involve the use of multi-temporal images to evaluate differences in (LULC) due to environmental conditions and human activities between the acquisition dates of images. The study area is a highly heterogeneous surface and 98.95 % is classified as bare land. LULC in this study map-to-map

comparison was adopted requiring that images from the three dates are classified, and then the three classified maps are compared. Map-to-map comparison is preferred for many applications as it can detect a full matrix of LULC changes for large amounts of data over large study areas such as the Ma'an Governorate, which occupied about 37% of the total area of Jordan. Based on Figure. 6 we can summarize the changes that occurred during the study period as the forest and irrigated area decreased by -11% from 1990 to 2000 and -97.1% between 2000-2018.

The movement rate was classified as high where it ranges between 5.2 and 7.7 m/y. 3. Moderate: sand dune movements in these areas are characterized by a rate of 3.3 to 5.50 m/y. This category dominates the areas with random distribution, it covers an area of 6863.8 km², 20.8%. 4. Low**:** the rate of movement in this category is low and fluctuated with accumulation in the base levels (Playa basins), and its movement ranges from 1.2.1 m/y, covering an area of 8777.7 km², 26.6% of the total area of Ma'an Governorate. It is estimated that most sand dune movement direction is towards the ESE, SE, SSE, and NW.

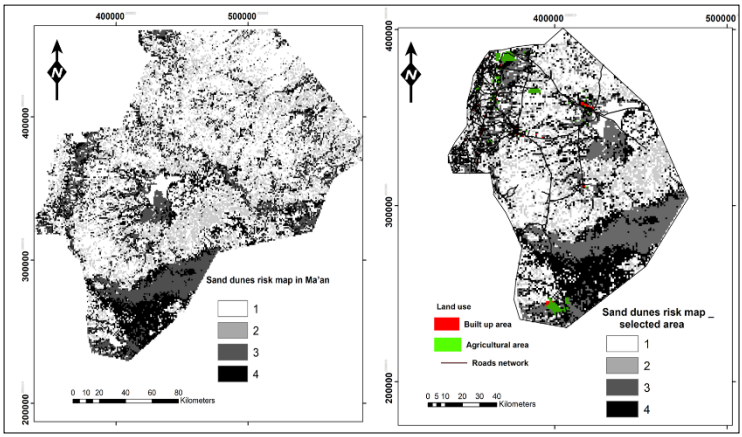

Figure 8: Sand dune hazard map in the study area, and the masked hazards map in the selected area

Table 6: Sand dune hazard affected in the study area by area and percentage

Risk level	Area (km²)	Area (%)
1 (Low)	8777.7	26.6
2 (Moderate)	6863.8	20.8
3 (High)	10955.7	33.2
4 (Very high)	6401.806	19.4
Total	32.999	100

As mentioned above, sand dunes represent 18.9% of the total area of Ma'an Governorate. The sand dunes are distributed in different areas in the study area, while the built-up area, the irrigated area, and the road network are highly concentrated in the western and southwestern region of the study area, within an area covering 15.764

km², 47.8%; 35.3% comprises sand stone rocks, and 25.1% is constituted of sand dunes. The study of sand dune movement will focus on explaining the impact of sand dunes on these human activities.

Table 7: Statistical characteristics of the selected site, according to Figure 8.

Risk level	Area km²	Area (%)
1(low)	3625	23
2 (Moderate)	1481	9.4
3 (High)	6621	42
4 (Very high)	4037	25.6
Total	15764	100

4. CONCLUSION

We concluded from the three images analyzed that sand dunes increased by 1.33km² and 8.63km² during the study period in the study area (see Table 3). The following is a study of the impact of the sand dunes in the urban area in detail. The rate of sand dune movement is controlled by wind speed, direction, slope, elevation, and land cover patterns. Movement rates were calculated. Most activities affected by sand dunes are concentrated in the western and southwestern areas, comprising the built-up area, irrigated area and the network of roads (see Figures 8-9). In 2018, the results showed that the study area, in

general, is exposed to a high risk of sand dune movement. The fieldwork and interviews with farmers showed that many farms were relocated from one place to another to avoid areas covered by sand dunes.

REFERENCES

AL-ANSARI, N., SALAMEH, E., & OMARI, H. (1990). "Analysis of rainfall in the Badia region". **Al al-Bayt University Research Paper**. Nº 1. Jordan.

AQL, M. (2002). "Movement of sands east Suez Canal and its impact on human activities: a study in applied geomorphology (In Arabic)". **Al-Ensaniat**. Vol. 19, pp. 1–75. Egypt.

EL-BAZ, F. (1998). "Sand accumulation and groundwater in the eastern Sahara". **Episodes**. Vol. 21, pp. 147–152. USA.

FADHIL, A. (2016). "Sand dunes monitoring using remote sensing and GIS techniques for some sites in Iraq". **The International Society for Optical Engineering**. Vol. 87, Nº 62. USA.

GAD, A. (2016). "Sand accumulation distribution and related impacts on agricultural resources of Sinai Peninsula". **Using integrated remote sensing-GIS techniques Global Advanced Research Journal of Agricultural Science**. Vol. 5, Nº 1: 42-50. Egypt.

HUGENHOLTZ, C, LEVIN, N., BARCHYN, T., BADDOCK, M. (2012). "Remote sensing and spatial analysis of aeolian Sand accumulations: A review and outlook". **Earth-Science Reviews**. Vol. 111, pp. 319-334. Netherlands.

JAMLI, A., ZAREKIA, S., & RANDHIR, O. (2018). "Risk assessment of Sand accumulation disaster in relation to geomorphic properties and vulnerability in the Saduq-Yazd Erg". **Applied ecology and environmental research**. Vol. 16, Nº 1: 579-590. Hungary.

KHIDR, M. (2006). "Aeolian forms and their hazards in the west of Wadi El- Arish: A geomorphological study". **Ph.D. Dissertation, Geography Department, Ain Shams University**. Egypt.

LIVINGSTONE, I., WIGGS, G., & WEAVER, C. (2007). "Geomorphology of desert Sand accumulations: A review of recent progress". **Earth-Science Reviews**. Vol. 80, pp. 239-257. Netherlands.

DEL ZULIA

opción

Revista de Ciencias Humanas y Sociales
Año 35, N° 24, (2019)

Esta revista fue editada en formato digital por el personal de la Oficina de Publicaciones Científicas de la Facultad Experimental de Ciencias, Universidad del Zulia.
Maracaibo - Venezuela

www.luz.edu.ve
www.serbi.luz.edu.ve
produccioncientifica.luz.edu.ve